



## **Roughness Investigation of SLM Manufactured Conformal Cooling Channels Using X-ray Computed Tomography**

**Klingaa, Christopher G.; Bjerre, Mathias K.; Baier, Sina; De Chiffre, Leonardo; Mohanty, Sankhya; Hattel, Jesper H.**

*Published in:*

Proceedings of the 9th Conference on Industrial Computed Tomography, Padova, Italy (iCT 2019)

*Publication date:*

2019

*Document Version*

Publisher's PDF, also known as Version of record

[Link back to DTU Orbit](#)

*Citation (APA):*

Klingaa, C. G., Bjerre, M. K., Baier, S., De Chiffre, L., Mohanty, S., & Hattel, J. H. (2019). Roughness Investigation of SLM Manufactured Conformal Cooling Channels Using X-ray Computed Tomography. In *Proceedings of the 9th Conference on Industrial Computed Tomography, Padova, Italy (iCT 2019)*

---

### **General rights**

Copyright and moral rights for the publications made accessible in the public portal are retained by the authors and/or other copyright owners and it is a condition of accessing publications that users recognise and abide by the legal requirements associated with these rights.

- Users may download and print one copy of any publication from the public portal for the purpose of private study or research.
- You may not further distribute the material or use it for any profit-making activity or commercial gain
- You may freely distribute the URL identifying the publication in the public portal

If you believe that this document breaches copyright please contact us providing details, and we will remove access to the work immediately and investigate your claim.

# Roughness Investigation of SLM Manufactured Conformal Cooling Channels Using X-ray Computed Tomography

Christopher G. Klingaa<sup>1,a</sup>, Mathias K. Bjerre<sup>1,b</sup>, Sina Baier<sup>2</sup>, Leonardo De Chiffre<sup>1</sup>, Sankhya Mohanty<sup>1</sup> and Jesper H. Hattel<sup>1</sup>

<sup>1</sup>Technical University of Denmark, Department of Mechanical Engineering, Produktionstorvet Building 425, Kgs. Lyngby, Denmark, e-mail: [cgkli@mek.dtu.dk](mailto:cgkli@mek.dtu.dk), [mathiasbjerre@gmail.com](mailto:mathiasbjerre@gmail.com), [ldch@mek.dtu.dk](mailto:ldch@mek.dtu.dk), [samoh@mek.dtu.dk](mailto:samoh@mek.dtu.dk), [jhat@mek.dtu.dk](mailto:jhat@mek.dtu.dk)

<sup>2</sup>Technical University of Denmark, Department of Physics, Fysikvej Building 307, Kgs. Lyngby, Denmark, e-mail: [sbaier@fysik.dtu.dk](mailto:sbaier@fysik.dtu.dk)

## Abstract

Conformal cooling channels are becoming one of the next big steps in the fabrication of moulds and tools. Mass flow rate and heat transfer are affected by the surface roughness in the cooling channels. The freeform shape of conformal cooling channels makes it difficult to evaluate the internal roughness with respect to classic planar techniques. This work presents a fitted-ellipse method to evaluate internal surface features of helical cooling channels. The investigated cooling channel was made from maraging steel 300 and manufactured with the selective laser melting process. X-ray computed tomography and image analysis were utilized in order to generate a freeform nominal surface by fitting ellipses to the reconstructed surface. The nominal surface was compared to the reconstructed surface and resulted in a point cloud of deviation values. The deviation values were used as input for deviation plots, inner area and volume estimations together with estimations of classic area surface parameters, according to ISO 25178-2:2012. Results showed that the internal surface features were highly orientation dependent, with extreme roughness observed on the downward facing surface of the cooling channel. The arithmetical mean height and average maximum height of the total inner surface were estimated at  $S_a = 13.7 \mu\text{m}$  and  $S_{z20} = 251 \mu\text{m}$ , respectively. The mass distribution was positively skewed, the root mean square height was  $S_q = 21.8 \mu\text{m}$  and the peaks observed on the surface were characterized as spiked. The obtained results suggested that the proposed method could evaluate the internal features of a helical cooling channel efficiently and qualitatively, while giving realistic quantitative estimations of the surface roughness characteristics.

**Keywords:** Conformal cooling channels, additive manufacturing, laser powder-bed fusion, computed tomography, roughness evaluation

## 1 Introduction

Capabilities of additive manufacturing are continuously improving and one of its key advantages over conventional manufacturing methods is the freedom of design and possibility of very complex geometries [1, 2]. The continuous progress seen within additive manufacturing and laser powder-bed fusion (LPBF) systems has enabled the manufacture of conformal cooling channels as an exciting next big step within the production of tooling systems. Conformal cooling channels have been shown to decrease cycle time, reduce residual stresses and warpage and increase accuracy of injection mould produced parts. This is due to a faster and more controlled cooling during manufacturing [1-3]. Nevertheless, additively manufactured conformal cooling channels are not challenge free. In order to build a closed cooling channel, the build itself will use powder as its support since added support structures would be difficult to effectively remove post manufacture [4]. This powder support tends to stick and partly melt together with overhanging surfaces [5]. Hence, characterization of cooling channel surfaces is an important aspect of accurately modelling and predicting the fluid flow and cooling ability of cooling channels. A change in friction factor and internal diameter may affect both mass flow rate due to pressure loss and change the effective heat transfer between fluid and channel wall [6]. This is already known and utilized in corrugated cooling channels. However, being able to accurately control and predict the cooling ability of a selective laser melting (SLM) produced cooling channel, requires knowledge of the expected internal surface features.

The overhanging areas of LPBF parts face significant challenges with roughness. Much research has been done within the investigation of roughness on overhanging sections of LPBF parts and the optimization of roughness by investigating the influence of common LPBF process parameters [5, 7, 8]. More often than not, classic roughness evaluations are made using profile analysis according to ISO 4288:1996 [9], giving parameters such as  $R_a$ ,  $R_q$  and  $R_z$ . Using profile characterization is intuitively adequate for linear features, in cases where this accurately describes the whole part. When a part has a complex geometry of multiple angled and rounded surfaces with orientation dependent features, profile characterization falls short. In order to fully characterize a surface, the number of required evaluations could be rather immense. Instead, the use of areal surface roughness parameters such as  $S_a$ , according to ISO 25178-2:2012 [10], together with CT measurements are gaining momentum [11, 12].

<sup>a</sup> Corresponding author

<sup>b</sup> Present address: Ørsted, Nesa Allé 1, 2820 Gentofte, Denmark



Classic planar techniques are not easily used for evaluating the internal roughness of freeform shapes [13]. Optical techniques are commonly used for areal characterization of the surface roughness, but have limitations in their ability to detect very steep slopes [14]. Large areas may be covered by stitching together topographs, but the complete characterization of SLM produced conformal cooling channels would require a large number of topographs. Finally, the method would require the channels to be cut into small pieces, possibly introducing error sources. For the areal analysis of additively manufactured components and internal features, research has instead moved towards the applicability of X-ray computed tomography (XCT or CT) for dimensional metrology [15]. With computed tomography, it is possible to non-destructively view and assess the internal features of parts, a unique capability currently possible with CT metrology only [16]. CT as a tool for metrology is still under development and a finished ISO standard has yet to be published [15]; instead, researchers look towards the German guideline VDI/VDE 2630 Sheet 1.2 for verifying the accuracy of the dimensional metrology measurements of a CT system [17]. Other methods include using the substitution method following the Guide to the expression of uncertainty in measurement (GUM) [18]. Some main areas in which CT scanning metrology is still facing significant hurdles are with respect to poor spatial resolution and completely understanding the error sources [11].

For roughness and deviation analysis of a CT scanned object, different approaches exist. Deviation analysis between a scanned object and a CAD file are possible in most post-processing software [16]. For objects with straight features such as straight cylinders, roughness and deviations are typically evaluated using a nominal surface obtained from a CAD model of the scanned object [19], but that is not done easily with freeform shapes. In order for the voxel size to be small enough to detect small features, an object may have to be scanned in several pieces. Dependent on the geometry of said object, it may be difficult or entirely impossible to properly align a CAD model with the scanned piece.

This work proposes a method for the evaluation of the inner surface roughness of SLM manufactured helical cooling channels. The ultimate goal of the current research is to predict and optimize the fluid flow and cooling ability of conformal cooling channels produced by SLM. In order to evaluate the internal roughness, it is proposed to use a fitted-ellipse approach as opposed to aligning a CAD file with the scanned object. Section 2 presents how a mesh was generated from a stack of fitted ellipses and used as a nominal surface of the cooling channel. The section furthermore describes how the deviation calculations between the nominal surface and the CT scanned surface was performed and utilized for surface evaluation, using areal roughness analysis according to ISO 25178-2:2012. Section 3 presents the deviation results and shows how the inner roughness was found to be highly orientation dependent and how the surface roughness was characterized as positively skewed and spiked. The suggested method is discussed in Section 4 in terms of the apparent accuracy of the method and its limitations. Finally, a conclusion and suggestions for future work are presented in Section 5.

## 2 Methods

The following section will describe the material and geometry of a SLM produced part used for roughness evaluation, the chosen CT scan strategy, the roughness analysis method and the computation of the roughness estimations.

### 2.1 Materials

The geometry of the part investigated in this work, was a helical cooling channel produced by the SLM process. The cooling channel was made in maraging steel 300. Figure 1 shows an overview of a test specimen developed with the purpose of testing the current capabilities of additive manufacturing systems [20]. From the multiple subparts found on the test specimen, the cooling channel investigated in this work is marked by the red dotted line. In order to get a representable part of the geometry,

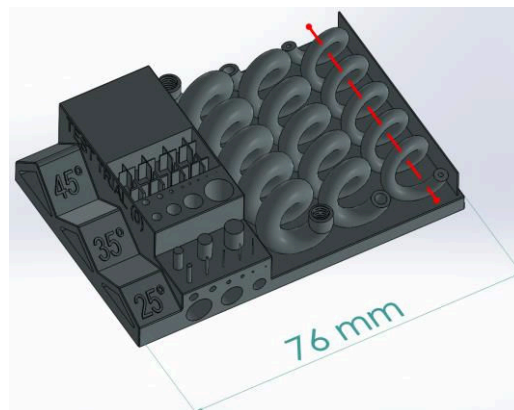


Figure 1: Test artefact for investigating capabilities of additive manufacturing systems [20]. The red dotted line marks the cooling channel that was investigated in this work.

the complete channel was cut from the test specimen using electrical discharge machining. Subsequently a smaller piece was cut from the channel using a saw. The smaller piece can be seen in Figure 2 mounted on a toothpick. The cut piece was one of the ends of the cooling channel and was used for CT scanning. The right side of the piece, as shown in Figure 2, was formerly connected to the rest of the cooling channel.



Figure 2: Cut cooling channel end-piece used for CT scanning.

## 2.2 CT Measurements

The CT scan of the cut piece was conducted using a ZEISS XRadia 410 Versa system. The X-ray tomograms were obtained by using a voltage of 150 kV, a power of 10 W and a HE3 filter. With a 4X objective and 2x2 binning, a voxel size of 3.55  $\mu\text{m}$  was obtained. The tomograms were recorded with 3210 projections and an exposure time of 18 s per projection. Reconstruction was done using an inbuilt reconstruction software package provided by ZEISS. The software uses filtered-back projection and is based on a Feldkamp, Davis and Kress algorithm [21]. Realignment, cropping and generation of TIFF images for roughness analysis were performed using Avizo 9.2. Figure 3 shows a cut-through section of the three dimensional representation of the reconstructed channel in xz orientation. The cropped and realigned section was subsequently exported as TIFF images in xy orientation. A visualization of the generated image stack can be seen in Figure 4. Each image had a resolution of 992 pixels by 1014 pixels and represented a cross-section of the channel in xy orientation. Due to the voxel size of 3.55  $\mu\text{m}$ , each slice represented a height of 3.55  $\mu\text{m}$  in the stacked direction.

The stack of images, extracted from the CT scanned volume shown in Figure 3, consisted of 996 images of which the inner 900 images were used for analysis due to CT artefacts in the outer images. This led to an evaluated image stack describing 3.195 mm in the stacked direction.

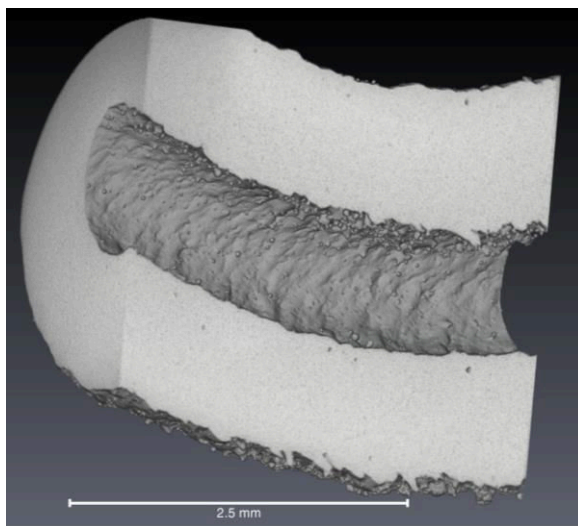


Figure 3: Section of the reconstructed channel, visualized in Avizo, showing the curvature of the channel.

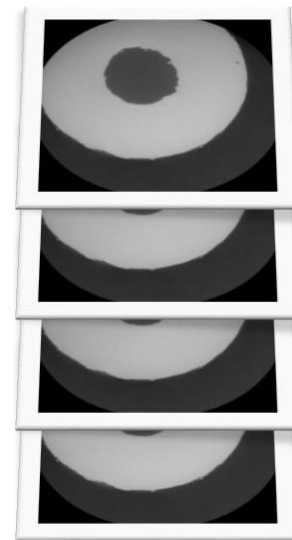


Figure 4: Visualization of the generated stack of images.

### 2.3 Method of Analysis

The analysis method suggested for investigating the roughness of helical cooling channels was based on a fitted geometry approach. An in-house Python code was developed with the purpose of analysing a complete stack of images automatically. In the following, the proposed approach is described.

Due to different intensities observed in the analysed images, the total stack of 900 images was divided into smaller stacks of 100 images each, where a better thresholding coherence within each stack was found. The stacks would then later be combined. The stacks of images were first loaded into ImageJ in order to obtain a segmentation threshold for each stack. Using the inbuilt “default” function for auto thresholding, the stacks of images were segmented into channel material and air. The “default” function is a variation of the IsoData approach introduced by Ridler and Calvard in 1978 [22, 23]. Subsequently the image stacks were loaded into the in-house Python code and analysed using the obtained segmentation thresholds. The fitted ellipse sequence may be followed in Figure 5(a) through 5(d). Only the internal channel was relevant for the analysis of internal surface roughness, thus the central void of each image was identified and isolated. The inner void was then cleaned from noise using the morphological image processes of image dilation followed by image erosion, in order to accurately fit a line on the contour of the void. An ellipse was then fitted to this contour using an algorithm developed by Fitzgibbon [24]. This way the fitted ellipse represented the underlying surface of the cooling channel wall and served as a nominal geometry.

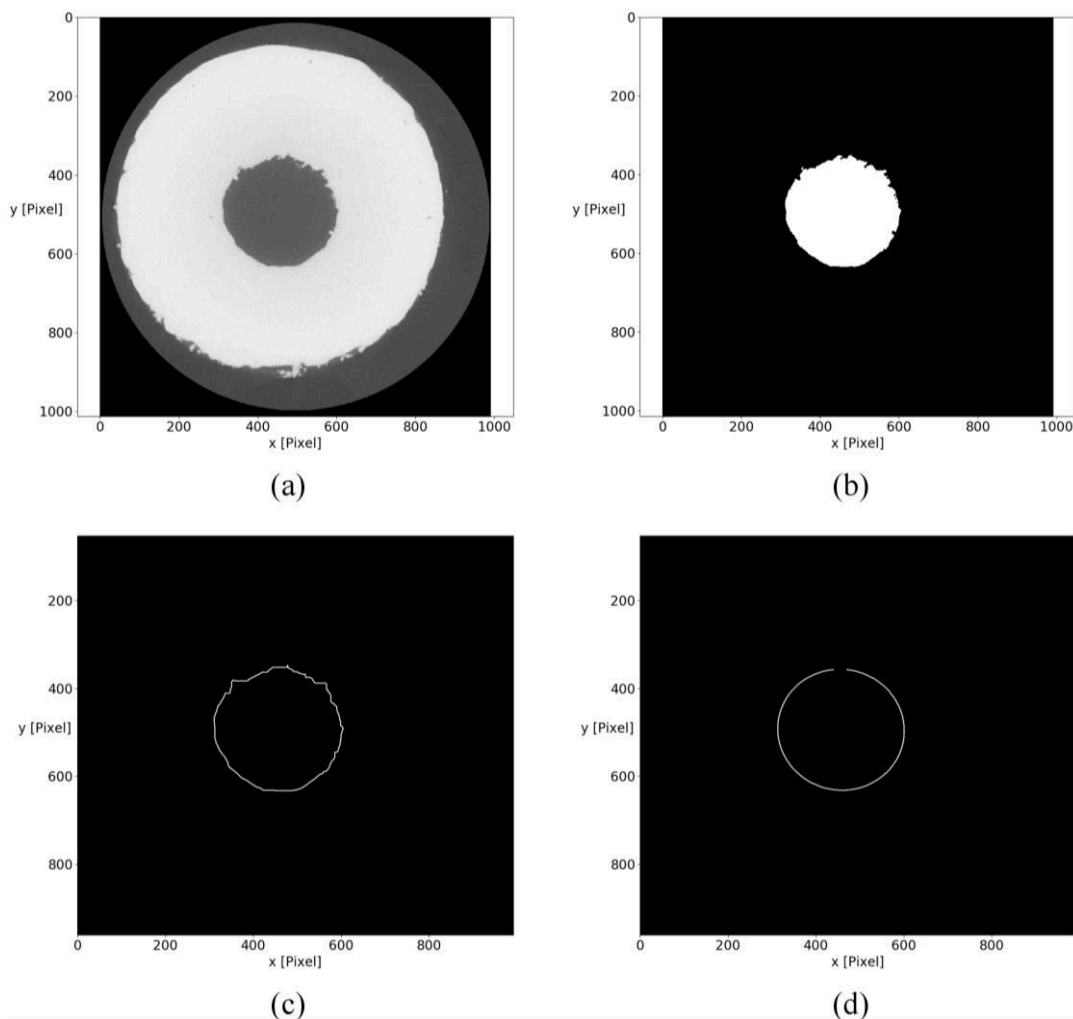


Figure 5: Overview of the generation of a fitted ellipse. (a) Original image slice. (b) Isolated inner void. (c) Generated contour after image dilation and subsequent erosion. (d) Final fitted ellipse.

This process was repeated for each slice, generating a stack of fitted ellipses. These ellipses were used to form a mesh representing the nominal surface of the channel. A mesh of the CT scanned surface was also generated. Both meshes were created using Lewiner’s optimization of the marching cubes method [25]. For each vertex on the CT meshed surface, the Euclidean distance between that point and all vertices on the meshed fitted ellipse surface was computed and the smallest distance was recorded as the deviation from the nominal surface. This yielded a 3D point cloud with a deviation value at each of the vertices of the meshed CT scanned surface.

## 2.4 Surface Texture Characterization

It was assumed that the nominal surface generated by the fitted ellipse approach represented a reference surface from which 3D roughness parameters would be calculated. Roughness estimations were calculated based on the ISO 25178-2:2012 standard. Due to the complex freeform geometry of the helical cooling channel, no filtering for form was conducted. The surface texture parameters selected for the characterization of the internal channel surface was the general height parameters and can be seen in Table 1.

Table 1: Overview of selected surface texture height parameters according to ISO 25178-2:2012.

Parameter	Equation
$S_a$ (Arithmetical mean height)	$S_a = \frac{1}{A} \iint_A  z(x,y)  dx dy$
$S_z$ (Maximum height)	$S_z = S_p + S_v$
$S_q$ (Root mean square height)	$S_q = \sqrt{\frac{1}{A} \iint_A z^2(x,y) dx dy}$
$S_{sk}$ (Skewness)	$S_{sk} = \frac{1}{S_q^3} \left( \frac{1}{A} \iint_A z^3(x,y) dx dy \right)$
$S_{ku}$ (Kurtosis)	$S_{ku} = \frac{1}{S_q^4} \left( \frac{1}{A} \iint_A z^4(x,y) dx dy \right)$
$S_p$ (Maximum peak height)	$S_p = \max(z(x,y))$
$S_v$ (Maximum valley height)	$S_v =  \min(z(x,y)) $

$S_a$  is the arithmetical mean height of the surface, compared to the mean plane of the surface, and gives a general description of the surface roughness over the area  $A$ .  $z(x,y)$  is the height value observed at a specific point.

$S_z$  is the maximum height observed in the sampling area. For this work, where the sampling area was the complete inner surface of the cooling channel, the computed  $S_z$  value was calculated as the average of the 10 largest heights, also denoted as  $S_{z20}$ .

$S_q$  is the root mean square height of the surface and is equivalent to the standard deviation of the height. This parameter describes the variation observed in the measured heights.

$S_{sk}$  represents the skewness of the observed surface. This parameter describes how the mass is distributed around the mean plane. If  $S_{sk} < 0$  most measurement points are above the mean plane, but the valleys are deeper than the peaks are high. If  $S_{sk} = 0$  the mass is evenly distributed around the mean plane. If  $S_{sk} > 0$  most measurement points are below the mean plane and the peaks are higher than the valleys are deep. In additive manufacturing, this parameter has been found to be able to help distinguish upskin from downskin (overhanging) surfaces [12].

$S_{ku}$  is a measure of the sharpness of the surface roughness. If  $S_{ku} < 3$  the surface consists of deep valleys and soft peaks. If  $S_{ku} = 3$  the surface has an equal distribution of sharp and soft valleys and peaks. If  $S_{ku} > 3$  the surface is characterized by a spiked

surface roughness.  $S_{ku}$  is an amplified version of the measure  $S_{sk}$ , but allows extremes to have a larger impact on the measure, thus giving a better indication of the sharpness of the roughness profile.

$S_p$  is the highest peak observed within the sampling area and  $S_v$  is the deepest valley observed within the same sampling area. Apart from areal roughness estimations, the in-house Python script also gave estimations of the inner surface area  $A_i$  and the volume of the channel cavity  $V_i$  as outputs.

Figure 6 shows a schematic overview of the proposed surface characterization methodology, from loading the image stack to calculation of the surface characterization parameters. An image stack is manually loaded into ImageJ and the Python code. After the threshold value has been obtained from ImageJ, it is given as an input in the Python code after which the image analysis and computation process is automated. 3D scatter plots of the CT scanned surface and the fitted ellipse surface are generated using the vertices of the meshed surfaces.

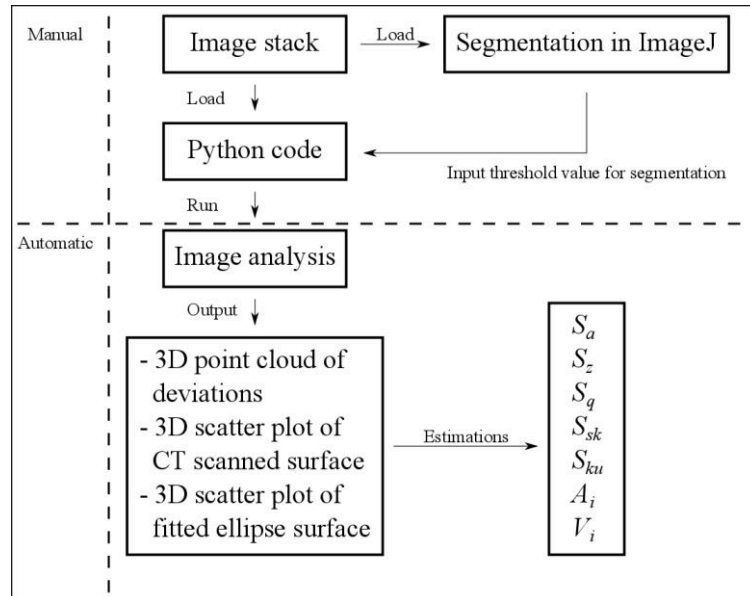


Figure 6: Schematic view of the proposed methodology for characterizing a conformal cooling channel.

### 3 Results

The generated fitted ellipses are shown in Figure 7 as a 3D scatter plot. The scattered points consist of the vertices from a mesh generated from 900 fitted ellipses. The scale is not the same on all axes since the x-axis and the y-axis were not constrained with the z-axis. This made the plot easier to view. The axes units were kept in pixels.

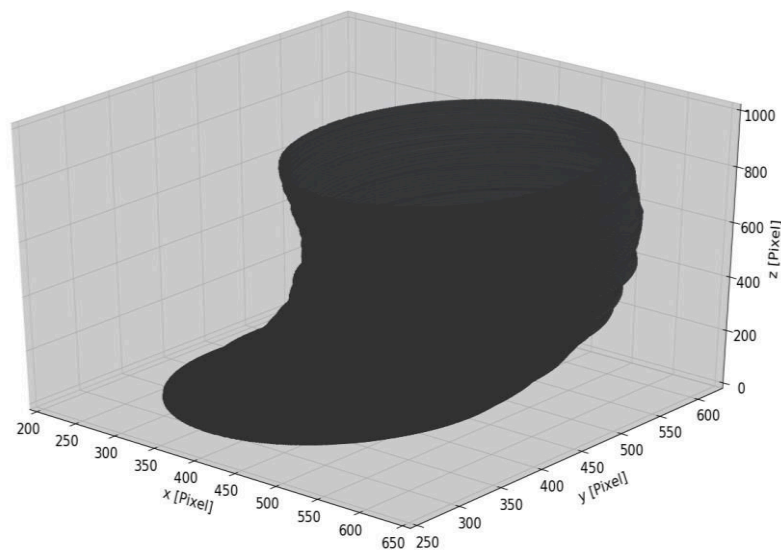


Figure 7: 3D scatter plot of vertices from the meshed fitted ellipse surface.

The deviation comparison between the fitted ellipse surface and the CT scanned surface is shown in Figure 8. Figures 8(a) and 8(b) show the same surface comparison, but at two different angles in order to visualize the 3D geometry. The top part of the Figures represents the right hand side of the CT scanned channel, shown in Figure 2 and visualized in Figure 3. The units on the axes were converted to mm using the obtained voxel size. The x-axis and the y-axis were not constrained with the z-axis, thus the scale is not the same on all axes. Figure 8 shows that the deviation values which were obtained by the comparison were widely distributed. It also shows how one side of the channel had higher deviation values. Table 2 shows an overview of the analysis results obtained from the surface deviation values. It must be noted that these calculations were carried out for the whole surface shown in Figure 8.

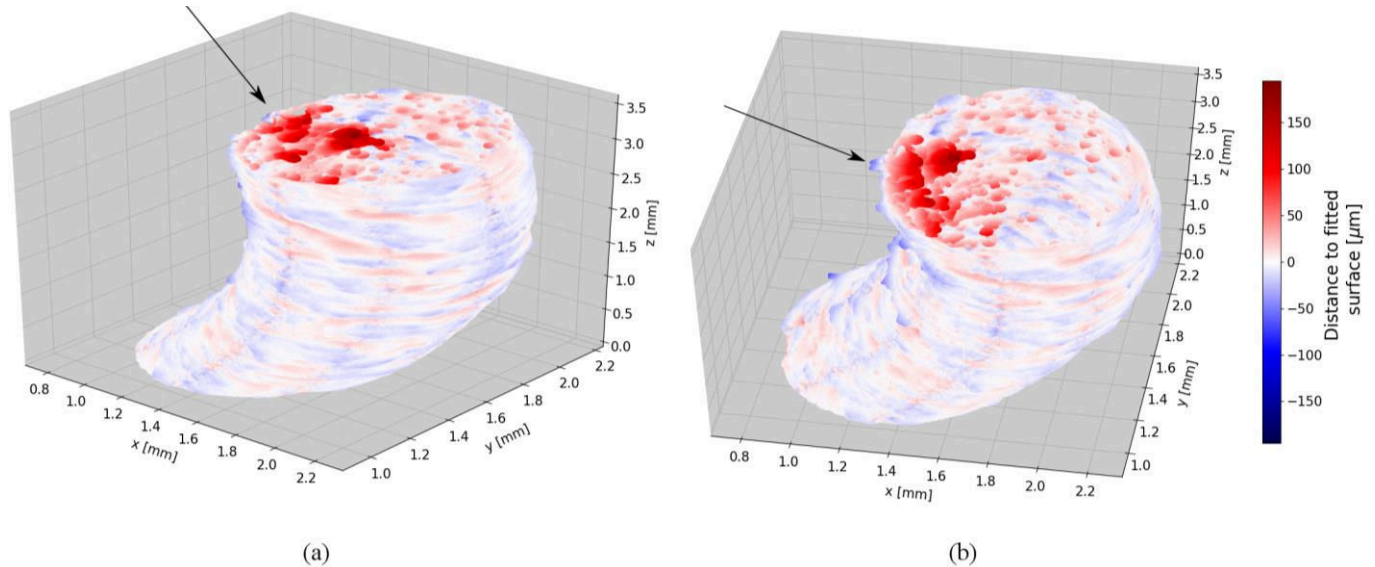


Figure 8: ((a), (b)) Snapshots of the deviation results taken at two different angles. The plots consist of 3D scatter plots of the vertices from the meshed CT scanned surface, together with the corresponding deviation values. Arrows mark the overhanging area of the cooling channel.

Table 2: Computed deviation results according to ISO 25178-2:2012 together with internal area and volume estimations.

Parameter	Estimation
$S_a$ (Arithmetical mean height)	13.7 $\mu\text{m}$
$S_{z20}$ (Average maximum height)	251 $\mu\text{m}$
$S_q$ (Root mean square height)	21.8 $\mu\text{m}$
$S_{sk}$ (Skewness)	2.88 [-]
$S_{ku}$ (Kurtosis)	13.0 [-]
$S_p$ (Maximum peak height)	189 $\mu\text{m}$
$S_v$ (Maximum valley height)	64.3 $\mu\text{m}$
$A_i$ (Internal wall area)	11.0 $\text{mm}^2$
$V_i$ (Internal volume)	2.49 $\text{mm}^3$

## 4 Discussion

In this section the results, the accuracy and the limitations of the proposed method are discussed.

### 4.1 Indications of Results and Their Accuracy

The arrows on Figure 8 mark the overhanging area of the cooling channel. The overhanging area showed high deviations and it is a well-known problem in LPBF that overhanging areas are experiencing high roughness. The surface deviation plots indicated a gradual decrease in the magnitude of deviations towards the part opposite to the overhanging area. Furthermore, the deviation values observed on the opposite half of the cooling channel surface, as compared to the overhanging area, were more evenly distributed.



The quantitative estimations could be used to further characterize the analysed surface. A  $S_a$  value of  $13.7 \mu\text{m}$  was estimated for the overall roughness of the cooling channel. This value is heavily affected by local deviations and thus this is generally not a good singular measure of the areal surface characteristics. The relationship between  $R_a$  and  $S_a$  is not easily described and is highly dependent on surface characteristics. Some work suggests that a linear relationship with a coefficient of close to 1 between the two factors can be found, as long as the surface primarily consists of non-directional features [26]. Other work shows that similar values may be mistakenly compared [27]. Under the assumption that  $R_a$  and  $S_a$  values are close but not equal, the values observed in this work were well within  $R_a$  values for as-made sand casted components, which typically range between  $12.5 \mu\text{m}$  and  $25 \mu\text{m}$ . In order to reach typical roughness values of components made by investment casting or die casting, the  $S_a$  value should be reduced by factors of 5 and 10, respectively [28]. Even though the  $S_a$  values might be comparable, a big difference between casted components and SLM manufactured components lies in the dependency on orientation. As visualized in Figure 8, the surface roughness of SLM manufactured cooling channels are highly orientation dependent. This confirms the still on-going challenges with respect to surface texture on SLM manufactured components as compared to conventional manufacturing techniques.

A  $S_{z20}$  value of  $251 \mu\text{m}$  was estimated. This confirms the large deviation values observed in Figure 8. This value was computed from the average distance between the 10 largest peaks and the 10 deepest valleys, thus the number was likely computed directly from the overhanging area and gave a good idea of the extremes observed.

A  $S_q$  value of  $21.8 \mu\text{m}$  was estimated, indicating a large variation in the observed surface deviations. This agreed well with the deviation variation visualized in Figure 8.

The estimated skewness value  $S_{sk}$  was 2.88. With reference to Section 2.4, this showed that most of the observed surface was below the mean surface, represented by the fitted ellipse surface. This characterized the surface as a surface with predominantly high peaks and shallow valleys. The estimated kurtosis value  $S_{ku}$  was 13.0. The high kurtosis indicated a general distribution of narrow and tall peaks. The plots shown in Figure 8 also confirmed this. For the extreme values, a maximum peak height  $S_p$  of  $189 \mu\text{m}$  and a maximum valley depth  $S_v$  of  $64.4 \mu\text{m}$  were estimated. The estimated inner area  $A_i$  was  $11.0 \text{ mm}^2$  and the estimated cavity volume  $V_i$  was  $2.49 \text{ mm}^3$ . As seen in Figure 2, the analysed section was close to straight. A straight cylinder of the same dimensions,  $D_i = 1 \text{ mm}$  and  $L = 3.195 \text{ mm}$  has an inner area of  $10.0 \text{ mm}^2$  and an inner volume of  $2.51 \text{ mm}^3$ . The difference in surface area could be due to the protruding and sunken features of the scanned surface. This may be important in relation to the cooling ability of the cooling channel since more surface area could be in contact with the fluid. The estimation of the inner volume was fairly close to that of a straight cylinder, indicating that the observed surface deviations had less influence on the overall volume of the channel cavity. The high kurtosis and extreme roughness may affect the cooling ability in cooling channels similar to the way that corrugated cooling channels have improved heat transfer as compared to straight channels [29].

The obtained results were difficult to compare with existing literature since no similar work was found. Roughness measurements are typically taken locally using conventional one-directional methods. One of the key advantages of using CT scanning and the proposed method of analysis is the possible investigation of internal features of freeform shaped conformal cooling channels. In order to do a similar investigation using conventional optical or probing techniques, one would have to cut the analysed section into many pieces and conduct an analysis on all separate pieces. This in itself would be very laborious and may introduce sources of error upon the measurements.

## 4.2 Limitations of the Proposed Methodology

The main limitation of the proposed method was related to the restrictions on the format of the analysed input. The image analysis process required each image to have a view of a completely enclosed elliptical shape in order to properly fit an ellipse. This meant that the CT scanned, reconstructed object needed to be aligned such that each image in the produced stack of images had a clear cross-sectional view of the cooling channel, before further processing. The length of the investigated section was heavily limited by the shape of the cooling channel. The smaller the turning angle of a helical cooling channel, the shorter a section must be, in order to have a cross-sectional view of the channel showing a fully enclosed channel. During the generation of fitted ellipses, the inner channel void was cleaned using image dilation and erosion. The kernel size used for this process may have effected the shape and placement of the fitted ellipses. A larger kernel could have a larger effect on smoothing out the extracted contour. Due to the 3D structures within the cooling channel, some features would show up on an image slice as a disconnected structure, some of these features were removed during the noise reduction and led to some of the largest protruding features not being fully with-taken during the fitting of an ellipse.

The focus of this research was on the development of a method for characterizing conformal cooling channels using non-destructive methods. The results were not made traceable, and even though the magnitude of the estimated roughness parameters was within an expected range, the quantitative values cannot be used until traceability of the results has been established.

The presented method may be dependent on the spatial resolution of the obtained CT scan. The voxel size must be small enough such that the most common surface features may be detected [30]. Voxel size also directly affects the meshed structure of the fitted ellipses. Larger voxel sizes lead to broader regions of interpolation between the fitted ellipses. This may introduce further error on the estimations. Furthermore, voxel size and surface roughness of a CT scanned part, has been found to influence dimensional analysis of CT scans [31]. Finally, the flow in channels are affected by protruding features along the flow direction and the apparent functionality of the 3D surface characterization parameters with respect to fluid flow are not yet clear.

## 5 Conclusion and Future Work

This work proposes a method for characterizing the internal surfaces of conformal cooling channels. The method yielded an overview of the surface feature distribution together with quantitative estimations of the surface area, the cavity volume and surface roughness parameters according to ISO 25178-2:2012. It was found that the proposed method was capable of efficiently giving a qualitative characterization and quantitative estimations of the surface texture characteristics of helical cooling channels. It may require several scans in order to fully characterize a channel geometry, but the amount of work required in order to achieve the same level of characterization by using optical or probing techniques is likely significantly larger. The investigated cooling channel was found to have a highly inhomogeneous roughness distribution with extremes found at the overhanging area of the channel. The surface was characterized as having a positive skewness, spiked peaks and a large variation in the observed deviations. With a working method for the characterization of internal surface features of SLM produced helical cooling channels, the current research has moved one step closer to accurately model and predict the flow and cooling ability of conformal cooling channels. The possibility of readily characterizing and evaluating additively manufactured cooling channels enables studies on the relationship between surface characteristics and production process parameters.

The method may be limited by the quality of the performed CT scans and future work is going to look into the influence of spatial resolution on the estimated surface characteristics. Furthermore, the functionality and traceability of the internal areal roughness estimations of the proposed method will be investigated.

### Acknowledgements

The Innovationsfond Grand Solutions project “MADE Digital” (grant no. 6151-000068) is thanked for funding this research. Professor Anders Bjornholm Dahl from the Department of Applied Mathematics and Computer Science at the Technical University of Denmark is thanked for supporting with the initial stages of the development of the image analysis Python code. The 3D Imaging Center at the Technical University of Denmark is gratefully acknowledged for their valuable support on X-ray computed tomography acquisition and image processing.

### References

- [1] M. K. Thompson, G. Moroni, T. Vaneker, G. Fadel, R. I. Campbell, I. Gibson, A. Bernard, J. Schulz, P. Graf, B. Ahuja and F. Martina, Design for Additive Manufacturing: Trends, opportunities, considerations, and constraints, *CIRP Annals*. 2016.
- [2] V. Petrovic, J. V. H. Gonzalez, O. J. Ferrando, J. D. Gordillo, J. R. B. Puchades and L. P. Grinan, Additive layered manufacturing: sectors of industrial application shown through case studies, *International Journal of Production Research*. 2011.
- [3] M. S. Shindea and K. M. Ashtankar, Additive manufacturing-assisted conformal cooling channels in mold manufacturing processes, *Advances in Mechanical Engineering*, 2017.
- [4] A. Voet, J. Dehaes, J. Mingneau, J. P. Kruth and J. Van Vaerenbergh, Laser Sintered Injection moulds, *Case Studies Made in Belgium*, PMI. 2015.
- [5] H. Chen, D. Gu, J. Xiong and M. Xia. Improving additive manufacturing processability of hard-to-process overhanging structure by selective laser melting. Elsevier. *Journal of Materials Processing Technology*, p. 99-108. 2017.
- [6] C. K. Stimpson, J. C. Snyder and K. A. Thole. Roughness Effects on Flow and Heat Transfer for Additively Manufactured Channels. ASME. *Proceedings of ASME Turbo Expo 2015: Turbine Technical Conference and Exposition*, June 15-19. 2015.
- [7] D. Wang, D. Xiao and Y. Yang. Surface quality of the curved overhanging structure manufactured from 316-L steel by SLM. Springer. *The International Journal of Advanced Manufacturing Technology*. 2016.
- [8] J. C. Fox, S. P. Moylan and B. M. Lane. Effect of process parameters on the surface roughness of overhanging structures in laser powder bed fusion additive manufacturing. Elsevier. *Procedia CIRP* 45. 2016.
- [9] ISO 4288:1996: Geometrical product specifications (GPS). Surface texture: Profile method – Rules and procedures for the assessment of surface texture.
- [10] ISO 25178-2:2012: Geometrical product specifications (GPS). Surface texture: Areal – Part 2: Terms, definitions and surface texture parameters.
- [11] A. Townsend, N. Senin, L. Blunt, R. K. Leach and J. S. Taylor. Surface texture metrology for metal additive manufacturing: a review. Elsevier. *Precision Engineering* 46, p. 34-47. 2016.
- [12] A. Triantaphyllou, C. L. Giusca, G. D. Macaulay, F. Roerig, M. Hoebel, R. K. Leach, B. Tomita and K. A. Milne. Surface texture measurement for additive manufacturing. IOP. *Surface Topography: Metrology and Properties*. 2015.
- [13] X. J. Jiang and D. J. Whitehouse, Technological shifts in surface metrology, *CIRP Annals - Manufacturing Technology*. 2012.
- [14] T. Vorburger. Optical Methods of Surface Measurement. National Institute of Standards and Technology (NIST). *Measurement Science and Standards in Forensic Firearms Analysis*. 2012.
- [15] Editors: S. Carmignato, W. Dewulf and R. Leach. *Industrial X-Ray Computed Tomography*. Springer. 2018.

- [16] J. P. Kruth, M. Bartscher, S. Carmignato, R. Schmitt, L. De Chiffre and A. Weckenmann. Computed tomography for dimensional metrology. Elsevier. CIRP Annals – Manufacturing Technology. 2011.
- [17] VDI/VDE 2630 Blatt 1.2. Computed tomography in dimensional measurement – Influencing variables on measurement results and recommendations for computed tomography dimensional measurements. The Association of German Engineers. 2018.
- [18] JCGM 100:2008. Evaluation of measurement data – Guide to the expression of uncertainty in measurement. Corrected version. 2010.
- [19] A. Du Plessis, I. Yadroitsev, I. Yadroitsava and S. G. Le Roux. X-Ray Microcomputed Tomography in Additive Manufacturing: A Review of the Current Technology and Applications. Mary Ann Liebert, Inc. 3D Printing and Additive Manufacturing. 2018.
- [20] M. Moshiri, G. Tosello and S. Mohanty, A new design for an extensive benchmarking of additive manufacturing machines, cuspen's 18<sup>th</sup> International Conference & Exhibition, Venice IT. June 2018.
- [21] L. A. Feldkamp, L. C. Davis and J. W. Kress. Practical cone beam algorithm. J. Opt. Soc. Am. A 1, 612-619. 1984.
- [22] ImageJ, Auto Threshold, [https://imagej.net/Auto\\_Threshold](https://imagej.net/Auto_Threshold). Accessed November 7. 2018.
- [23] "Picture Thresholding Using an Iterative Selection Method," in IEEE Transactions on Systems, Man, and Cybernetics, vol. 8, no. 8, pp. 630-632. August 1978.
- [24] A. W. Fitzgibbon and R. B. Fisher, *A buyer's guide to conic fitting*, Proceedings of the 6<sup>th</sup> British Machine Vision Conference 1995, Vols 1 and 2, p. 513-522. B M V A PRESS. 1995.
- [25] T. Lewiner, H. Lopes, A. Vieira and G. Tavares. Efficient Implementation of Marching Cubes' Cases with Topological Guarantees. Journal of Graphics Tools. 2012.
- [26] M. Harcarik and R. Jankovych. Relationship between values of profile and areal surface texture parameters. MM Science Journal. 2016.
- [27] F. Blateyron. Does it make sense to compare Ra and Sa values. <https://www.digitalsurf.com/blog/does-it-make-sense-to-compare-ra-and-sa-values/>. Accessed November 14, 2018.
- [28] E. P. DeGarmo, J. T. Black and R. A. Kohser. Materials and processes in manufacturing, 9th ed., International ed.), Wiley, New York, Chichester. 2003.
- [29] E. A. M. Elshafei, M. M. Awad, E. El-Negiry and A. G. Ali. Heat transfer and pressure drop in corrugated channels. Elsevier. Energy. 2009.
- [30] L. De Chiffre, S. Carmignato, J. P. Kruth, R. Schmitt and A. Weckenmann. Industrial applications of computed tomography. Elsevier. CIRP Annals – Manufacturing Technology. 2014.
- [31] S. Carmignato, V. Aloisi, F. Medeossi, F. Zanini and E. Savio, Influence of surface roughness on computed tomography dimensional measurements, CIRP Annals – Manufacturing Technology, p. 499-502. 2017.